

# RECONSTRUCT TRANSVERSE INITIAL CONDITIONS OF HIGH INTENSITY BEAMS USING MACHINE LEARNING

H. D. Zhang<sup>\*,1,2</sup>, Q. Xu<sup>1,2,3</sup>, C. P. Welsch<sup>1,2</sup>

<sup>1</sup>University of Liverpool, Liverpool, UK

<sup>2</sup>Cockcroft Institute, Warrington, UK

<sup>3</sup>CERN, Geneva, Switzerland

## Abstract

Space charge effect was considered a driving force for emittance growth in high-intensity beams. To understand it, the emittance needs to be measured. In the past, the quadrupole scan was one of the simple and efficient methods to measure beam emittance, but it is difficult to apply to high-intensity beams where the space charge plays a dominant role due to the deviation from the quadratic fitting. The tomography method was used before for this case to reconstruct phase space and then obtain the emittance, but the scan was time-consuming, and the post-analysis is very complex. One of the solutions is to use the genetic algorithm and treat this as an optimisation problem where the emittance needs to be optimised for the beam to match the quadrupole scans. This method also involves heavy post-analysis, which limits its online application.

In this contribution, machine learning methods will be used to reconstruct the transverse initial conditions based on PIC simulations of space charge-dominated beams. The effectiveness of the machine learning method against the space charge level will be studied.

## INTRODUCTION

Transverse emittance is a key quality factor for particle beams in accelerators. Knowing it precisely will help control the machine and avoid beam loss. Traditionally, it was measured by methods such as a quadrupole scan, a multi-slit, and a pepper pot. Other novel methods [1] have also been applied. Due to its simplicity, the quadrupole scan method was widely used in many accelerator facilities. It utilizes one quadrupole and a beam profile monitor, which can be invasive, such as scintillating screens, optical transition screens, or secondary emission monitors, or non-invasive, such as synchrotron radiation monitors, gas-based ionization, or beam-induced fluorescent monitors. The method relies on varying the quadrupole field and recording the beam sizes. Based on the linear transfer matrix, the measured beam size square can be fitted in a quadratic form associated with the varying quadrupole strength, where initial conditions such as beam size, beam slope, and emittance can be obtained from the coefficients of the quadratic function.

However, in high-intensity beams, space charge plays an important, if not dominant, role, and the transfer matrix cannot be decoupled from the beam sizes and even becomes nonlinear in extreme cases, thus the fitting from the quadrupole

scan will overestimate the emittance compared with the measurement by a more precise method, such as multi-slits and simulations [2]. Previously, optimization methods were used to resolve the emittance for space-charge-dominated beams, including particle swarm [3] and genetic algorithms [4]. Those methods tried to solve the initial condition by optimizing them to fit the quadrupole scan data using a linear space charge model when describing the envelope evolution over time. Those methods are effective, but the post-process is very time-consuming.

In this paper, a machine learning method, specifically the regression model, is proposed to obtain the emittance from the quadrupole scan data for high-intensity beams. The space charge level, as well as the effective measurement range of emittance, will be discussed using the quadrupole scan data from particle-in-cell simulations.

## METHOD

### Dataset Generation

The beam envelope equation in Eqs. (1) and (2) describes beams with linear space charge force in a non-accelerating environment.

$$X'' + k_x X - \frac{2K}{X+Y} - \frac{\epsilon_x^2}{X^3} = 0, \quad (1)$$

$$Y'' + k_y Y - \frac{2K}{X+Y} - \frac{\epsilon_y^2}{Y^3} = 0, \quad (2)$$

where  $X, Y$  are the horizontal and vertical envelopes of the beam (two times of the rms size),  $k_x, k_y$  are the external force strength in the x and y direction separately,  $K$  is the dimensionless generalized permeance, indicates a space charge level, and  $\epsilon_x, \epsilon_y$  are the effective emittances in the x and y direction separately. These equations are derived from the single-particle trajectory equation, considering the linear space charge force from a K-V distribution. Still, they can be extended to other distributions in terms of the RMS value. When  $K \lesssim 10^{-6}$ , the space charge can be ignored; when  $10^{-6} \lesssim K \lesssim 10^{-4}$ , the space charge is moderate; when  $K \gtrsim 10^{-4}$ , the beam can be considered as space-charge dominant.

To use the quadrupole scan data for emittance or initial condition reconstruction, a simple case was considered, as shown in Fig. 1. High-intensity beam with initial conditions including beam sizes ( $X_0, Y_0$ ), beam slopes ( $Xp_0, Yp_0$ ), and beam emittances ( $\epsilon_{x0}, \epsilon_{y0}$ ) propagates through the quadrupole scan system, which includes a drift with

\* haozhang@liverpool.ac.uk

length  $D$ , a quadrupole with strength  $k$  and effective length  $L$ , and second drift with length  $D$  to reach the location of the screen at  $s = 2D + L$ . In this simulation, a setting that is close to UMER [5] conditions is used with an electron beam at the energy of 10 keV. The space charge level indicated by  $K$  and associated with the beam current and energy is shown in Table 1. For each beam current, one input dataset was defined as an array of the final beam sizes ( $X_1, X_2, \dots, X_{41}, Y_1, Y_2, \dots, Y_{41}$ ) in 41 quadrupole settings. The output dataset is an array of the 6 initial conditions ( $X_0, Y_0, X_{p0}, Y_{p0}, \epsilon_{x0}, \epsilon_{y0}$ ). To create the datasets, the initial conditions are generated using a logarithmic uniform random function within upper and lower bounds (200 mm, 0.02 mm) for beam sizes, ( $\pm 200$  mrad,  $\pm 0.02$  mrad) for the beam slopes, and (100 mm mrad, 0.01 mm mrad) for the beam emittances. The final beam sizes at the screen for a quadrupole scan can be obtained by solving Eq.(1, 2) with given initial conditions, space-charge level, and a set of quadrupole strengths ( $k_1, k_2, \dots, k_{41}$ ). A desktop with an Intel Core i9 9900k, 32 GB DDR4 memory was used to generate 100k datasets by solving the envelope equations in MATLAB.

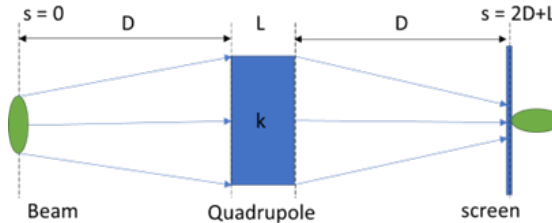


Figure 1: Illustration of a quadrupole scan system.

Table 1: Space Charge Level of Simulated Electron Beam

Beam Current $I$ (mA)	Generalized Perveance $K$
0.6	$8.96 \times 10^{-6}$
6.0	$8.96 \times 10^{-5}$

### Reconstruction Model and Its Training

A regression architecture is used as the training model, as shown in Fig. 2. It uses a 3-layer fully connected neural network. Each layer applied a ReLU activation to improve gradient stability during training, except the output layer, since the regression model outputs continuous values.

The neural network model was developed using PyTorch and trained on the same desktop with a graphics card of NVIDIA GeForce RTX 3090 with 10,496 CUDA cores. The Adam algorithm was used to optimize the model with a learning rate of 0.0001. 5000 epochs are used, but the training converges very quickly. For model evaluation, 30% of the total 100k datasets were randomly partitioned for evaluation. The mean squared error (MSE) was used as the loss function.

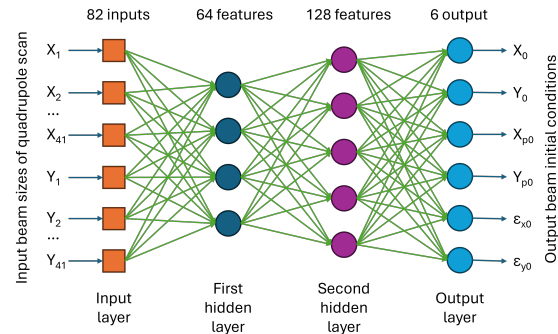


Figure 2: Architecture of the regression neural network for beam initial condition reconstruction from a quadrupole scan. It has two hidden layers with 64 neurons and 128 neurons each.

### Test Data Generation (WARP)

To test the model trained, a quadrupole scan of the same beam condition was simulated using a Particle-In-Cell (PIC) code WARP [6]. A slice field solver (wxy) was used in the WARP simulation, which treats the beam as an infinitely long bunch; thus, the longitudinal space charge effect is not considered. The default initial conditions of the beams are listed in Table 2. To compare different ratios of space charge and emittance, the quadrupole scan for each beam with a different current was simulated in WARP with varying values of emittance from 0.01 to 100 mm mrad.

Table 2: Default Initial Condition of UMER-Like Beams

Current $I$ (mA)	Size $X_0(Y_0)$ (mm)	Slope $X'_0(-Y'_0)$ (mrad)	Emittance $\sigma_x(\sigma_y)$ (mm mrad)
0.6	1.60	7.50	5.00
6.0	3.20	15.00	15.00

## RESULTS

### Training Results

The predicted parameters against the 30% test data for the 6 mA beam were shown in Fig. 3. The scattered points for beam sizes closely follow a straight line with a unit slope, indicating a strong agreement between the predicted and actual values. The beam slope prediction is not as good as the beam sizes, but still fairly follows the unity slope line. However, the predicted emittances have huge errors. For the y-emittance, although the predicted data were scattered around the unit slope line, they still show a good prediction trend. While for the x-emittance, the predicted data show two competing modes, which are currently not fully understood. This phenomenon also happens for the 0.6 mA beam. Possible reasons are the small initial sizes and emittances used in both training and test data, which are not representative of physical and flawless conditions.

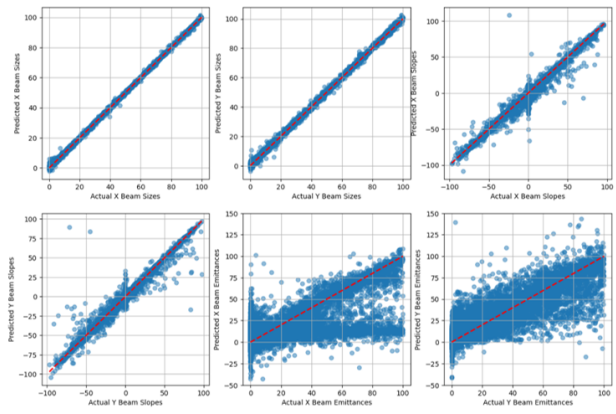


Figure 3: Prediction of the initial conditions over the test set of data for beam sizes, divergences, and emittances.

Table 3: Prediction of the Initial Condition From the WARP Simulated Quadrupole Scan

Parameters	Values	
Beam current $I$ (mA)	0.6	6
Size $X_0/Y_0$ (mm)	1.6/1.6	3.2/3.2
Regression model (mm)	1.22/2.37	3.09/4.30
Slope $X'_0/Y'_0$ (mrad)	7.5/-7.5	15.0/-15.0
Regression model (mrad)	7.61/-6.01	14.90/-14.54
Emittance $\epsilon_{x0}/\epsilon_{y0}$	5.0/5.0	15.0/15.0
Regression model (mm mrad)	4.991/1.07	10.02/8.22

### Test with WARP Simulations

As suggested by [4], a typical quadrupole scan of a UMER-like beam with 6 mA current and 10 keV energy will give an imaginary value of emittance and indicate that the quadrupole scan method is invalid when the transverse space charge force is dominant. Using the trained model, we can predict the initial conditions, shown in Table 3. Clearly, the model can be used to indicate the beam size and divergence very well, and for emittances, the error is as large as 40%. Figure 4 shows that when the emittance is smaller than 3 mm mrad, the emittance remains constant as 3 mm mrad. One reason was concluded to be that when the emittances are small compared to the space charge force, they will grow during the quadrupole scan section. This effect was included in the PIC WARP simulation but not included in the MATLAB envelope solver that generated the training data. This can be seen from the WARP simulation for the small emittance cases, the sizes for the quadrupole scan are almost indistinguishable. If this model were applied to the real data to predict the small emittance, the accuracy of the measurement would be very demanding and sometimes impossible.

When compared with the advanced algorithm, the regression neural network has its own benefit when swap-

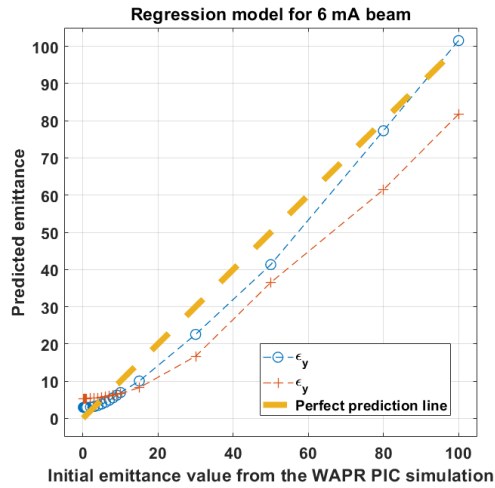


Figure 4: Prediction of the initial emittances over the WARP simulated quadrupole scan.

ping the WARP simulation data to a real measurement quadrupole scan. Firstly, the advanced algorithm is a post-process method, which optimises the initial conditions to fit the quadrupole scan data. The data processing normally takes a long time and thus cannot give a prediction in real time. In contrast, the neural network methods are based on pre-simulated data and a trained model with them. Applying the model normally takes negligible time, and thus, real-time emittance prediction after a quadrupole scan is possible.

## CONCLUSION

In summary, a machine learning framework for a quadrupole scan has been set up for a space-charge-influenced beam. Data obtained from both the 0.6 mA (space charge affected) and 6 mA (space charge dominated) beams are used to construct a regression neural network. Currently, this method shows a potential for initial condition prediction. It is good at predicting initial beam sizes and beam divergences, but when predicting the emittance, especially for small emittance values, the error is still large, which is due to the limitation of how the data is generated, where emittance growth is not considered in the MATLAB calculation. In the next step, instead of only solving the envelope equation with a conserved emittance value, the PIC code will be used to more accurately simulate the quadrupole scan in various initial conditions. That data can be simulated before a quadrupole scan of a space-charge-influenced beam to create and evaluate the model. Real experimental data, such as from UMER, could be used for testing how the simulation-based model behaves in a real beam environment.

## ACKNOWLEDGEMENTS

This work was supported by the Cockcroft core grant no. ST/G008248/1.

## REFERENCES

[1] K. Poorrezaei, R. B. Fiorito, R. A. Kishek, and B. L. Beaudoin, “New technique to measure emittance for beams with space charge”, *Phys. Rev. Spec. Top. Accel. Beams*, vol. 16, no. 8, p. 082801, Aug. 2013.  
[doi:10.1103/PhysRevSTAB.16.082801](https://doi.org/10.1103/PhysRevSTAB.16.082801)

[2] S. G. Anderson, J. B. Rosenzweig, G. P. LeSage, and J. K. Crane, “Space-charge effects in high brightness electron beam emittance measurements”, *Phys. Rev. Spec. Top. Accel. Beams*, vol. 5, no. 1, p. 014201, Jan. 2002.  
[doi:10.1103/PhysRevSTAB.5.014201](https://doi.org/10.1103/PhysRevSTAB.5.014201)

[3] A. D. Stepanov *et al.*, “Optimizing beam transport in rapidly compressing beams on the neutralized drift compression experiment-II”, *Matter Radiat. Extrem.*, vol. 3, no. 2, pp. 78–84, Feb. 2018. [doi:10.1016/j.mre.2018.01.001](https://doi.org/10.1016/j.mre.2018.01.001)

[4] H. D. Zhang and C. P. Welsch, “Simulation study of emittance measurement using a genetic algorithm for space charge dominated beams”, in *Proc. IPAC’21*, Campinas, Brazil, May 2021, pp. 935–938.  
[doi:10.18429/JACoW-IPAC2021-MOPAB295](https://doi.org/10.18429/JACoW-IPAC2021-MOPAB295)

[5] RA. Kishek *et al.*, “The University of Maryland electron ring program”, *Nucl. Instrum. Methods Phys. Res. A*, vol. 733, pp. 233–237, 2014. [doi:10.1016/j.nima.2013.05.062](https://doi.org/10.1016/j.nima.2013.05.062)

[6] A. Friedman *et al.*, “Computational methods in the Warp code framework for kinetic simulations of particle beams and plasmas”, *IEEE Trans. Plasma Sci.*, vol. 42, no. 5, pp. 1321–1334, 2014. [doi:10.1109/TPS.2014.2308546](https://doi.org/10.1109/TPS.2014.2308546)